Langmuir

Article

pubs.acs.org/Langmuir

Highly Sensitive Detection of Surface and Intercalated Impurities in Graphene by LEIS

Stanislav Průša,[†,‡] Pavel Procházka,[†,‡] Petr Bábor,[†,‡] Tomáš Šikola,[†,‡] Rik ter Veen,[§] Michael Fartmann,[§] Thomas Grehl,[∥] Philipp Brüner,[∥] Dietmar Roth,[⊥] Peter Bauer,[⊥] and Hidde H. Brongersma*[,§,∥]

[†]Institute of Physical Engineering, Brno University of Technology, Technická 2896/2, 61669 Brno, Czech Republic

[‡]CEITEC BUT, Brno University of Technology, Technická 3058/10, 61600 Brno, Czech Republic

[§]Tascon GmbH, Mendelstr. 17, 48149 Münster, Germany

[∥]ION-TOF GmbH, Heisenbergstr. 15, 48149 Münster, Germany

[⊥]Institute of Experimental Physics, Johannes Kepler University Linz, Altenberger Straße 69, A-4040 Linz, Austria

Supporting Information

ABSTRACT: Low-energy ion scattering (LEIS) is known for its extreme surface sensitivity, as it yields a quantitative analysis of the outermost surface as well as highly resolved in-depth information for ultrathin surface layers. Hence, it could have been generally considered to be a suitable technique for the analysis of graphene samples. However, due to the low scattering cross section for light elements such as carbon, LEIS has not become a common technique for the characterization of graphene. In the present study we use a high-sensitivity LEIS instrument with parallel energy analysis for the characterization of CVD graphene transferred to thermal silica/silicon substrates. Thanks to its high sensitivity and the exceptional depth resolution typical of LEIS, the graphene layer closure was verified, and different kinds of contaminants were detected, quantified, and localized within the graphene structure. Utilizing the extraordinarily strong neutralization of helium by carbon atoms in graphene, LEIS experiments performed at several primary ion energies permit us to distinguish carbon in graphene from that in nongraphitic forms (e.g., the remains of a resist). Furthermore, metal impurities such as Fe, Sn, and Na located at the graphene−silica interface (intercalated) are detected, and the coverages of Fe and Sn are determined. Hence, high-resolution LEIS is capable of both checking the purity of graphene surfaces and detecting impurities incorporated into graphene layers or their interfaces. Thus, it is a suitable method for monitoring the quality of the whole fabrication process of graphene, including its transfer on various substrates.

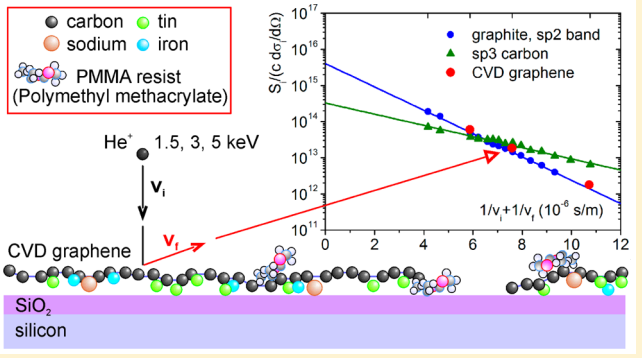

1. INTRODUCTION

An optimal graphene structure exhibits unique electronic properties such as very low electrical resistance, extremely high carrier mobility,[1] ferromagnetic properties,[2] and unprecedented mechanical strength.[3] This has generated new applications such as gas sensors and biosensors,[4−6] THz transistors,[7] light detectors and solar cells,[3,8] and graphene-based membranes.[9] However, the performance and reliability of the properties of these devices are generally negatively affected (degraded) by defects in the graphene layer or by surface impurities and impurities at the interface between the monolayer of graphene and the substrate (intercalated). While the structural defects (point and line defects)[10] influence the mechanical and electronic properties,[11,12] contamination due to surface and intercalated impurities almost exclusively affects the electronic properties.[13] A serious effort was made to optimize the CVD graphene transfer to the desired substrates as well as to chemical- and annealing-based cleaning and monitoring of the graphene contamination.[14−17] Although graphene is an ideal representative of 2D materials, it has a specific thickness defined by two external interfaces. For instance, wet transferred CVD graphene[18] is generally affected by residual resists on the top side[11] and by metal contaminants at both interfaces and in interstitial positions.[12]

Integral information about graphene and its defects and contamination is rather easily obtained by standard analytical methods such as Raman spectroscopy (RS) and X-ray photoelectron spectroscopy (XPS). However, since graphene is investigated as a one-atomic-layer-thick or few-atomic-layers-thick material, the analysis is hampered by the much larger depth of information of most analytical techniques. A reliable analytical technique for the detection and quantification of these ultrathin layers and its impurities is critically lacking in this emerging research area.

Received: May 30, 2015
Revised: July 21, 2015
Published: July 22, 2015

DOI: 10.1021/acs.langmuir.5b01935
Langmuir 2015, 31, 9628−9635

Low energy ion scattering (LEIS) is known for its extreme surface sensitivity. It gives a quantitative analysis of the outermost surface as well as highly resolved in-depth information for ultrathin layers.[19,20] Since at low energies (1−10 keV) the scattering cross sections scale with the atomic number, the sensitivity for a light element such as carbon is relatively poor for standard LEIS. Due to the fact that He^+ ions are detected in LEIS, the scattered ion energy is low as a result of the low mass ratio for this target-projectile combination. The resulting low velocity of the scattered He^+ at its outgoing trajectory results in a very effective neutralization and thus in a particularly low LEIS signal. An additional problem is that carbon is a common contaminant in surface analysis, while it is also known that the surface of graphene is susceptible to contamination by resist residues[21] and other organic molecules. Thus, for a reliable study it is crucial to be able to distinguish the carbon related to such a contamination from the carbon in graphene. Since the atomic sensitivities for LEIS are, in general, independent of the neighboring atoms ("absence of matrix effects"),[20] one might be tempted to exclude LEIS as a useful analysis technique for graphene characterization. In fact, there has been no systematic LEIS study of graphene published until now.

For graphitic and carbidic carbon, however, an exceptionally strong matrix effect has been observed.[22,23] In the present study this matrix effect is exploited to distinguish graphene carbon from other types of carbon representing graphene contaminants. The unique electronic structure of graphene (and graphite) causes an exceptionally strong neutralization of the backscattered helium ions. At the lowest primary energy (1.5 keV), where the interaction time between helium and carbon is longest, the neutralization by graphene is so strong that the signal of backscattered ions is virtually undetectable. Other types of carbon do not show this effect. At the highest primary energy (10 keV) both the neutralization by graphene and nongraphene carbon are much smaller and the LEIS signals are comparable. By combining LEIS analyses at several energies, this matrix effect can be used to distinguish and quantify the surface coverage by graphene carbon and by other types of carbon.

The impact of the ions used for the analysis will lead to sputtering and will thus produce carbon vacancies,[24] which will locally change the electronic structure of graphene.[25] Thus, notwithstanding the low sensitivity for carbon, it is still crucial to use such a low ion fluence that the created damage is negligible (static LEIS).

Herein we report the use of high-sensitivity (HS) LEIS with parallel energy analysis and time-of-flight (ToF) filtering for background reduction (Qtac 100). Typical for such a dedicated HS-LEIS instrument is the very large solid angle for the detection of the backscattered ions at a well-defined large scattering angle (145°). As a result, the sensitivity limit has been significantly improved (down to 10^{-5} monolayers) compared to the classical LEIS instrumentation. The instrument can also cover the full energy range of LEIS, which is a prerequisite for the present study. To demonstrate the instrument's efficiency, the presented spectra can be compared to a spectrum (scattered ions detected together with neutralized projectiles and sputtered particles) that results from the analysis of a similar graphene sample by a conventional time-of-flight LEIS spectrometer[26] in the Supporting Information.

The extraordinarily strong neutralization of He^+ ions by graphene can be explained in terms of the quasi-resonant charge transfer of an electron from the very wide energy band of graphene to the helium 1s vacancy (see section below).

2. EXPERIMENTAL SECTION

2.1. Materials. The following materials were used as reference samples for the LEIS experiments: highly oriented pyrolytic graphite (HOPG; Goodfellow GmbH, Germany) and silicone rubber $[-Si-O-(CH_3)_2-]_n$.

2.2. Graphene Sample Preparation. The graphene layer is grown by a standard CVD procedure[18] from methane on a copper foil of high purity (99.99%, MTI Corporation). Subsequently, the graphene is transferred onto a silicon substrate (Si(111) phosphorus doped, covered by a 3-nm-thick native oxide layer) via the following steps: the front side of the graphene is spin coated with 350 nm poly(methylmethacrylate) (PMMA), and then the graphene on the back side of the copper foil is etched away by oxygen/argon plasma. After the copper foil is dissolved by wet etching in an iron(III) nitrate solution ($Fe(NO_3)_3{\cdot}9H_2O$), the graphene−PMMA sandwich is pulled out of the solution and immersed several times in a freshwater bath (deionized water, conductivity <0.5 μS/cm).

The graphene−PMMA sandwich is taken out of the final bath, placed on a silicon substrate, and air dried. The PMMA layer is removed by acetone and IPA. After that the sample surface is rinsed in H_2O and blown dry with nitrogen.

2.3. Experimental Equipment. LEIS measurements are carried out using a Qtac 100 (ION-TOF GmbH, Münster, Germany). In this high-resolution, high-sensitivity low-energy ion scattering (LEIS) instrument a normal incidence ion beam (E_i = 1−8 keV) is used to generate scattered ions. The double-toroidal analyzer with full azimuthal acceptance uses parallel energy detection for maximum sensitivity. At the same time the polar scattering angle (145°) and angular resolution are chosen for high mass resolution.

Essential to low detection limits, especially light elements, is the suppression of the background from sputtered ions such as hydrogen. Using a pulsed primary beam and ToF filtering system, we can identify and remove from the spectrum ions with different mass than that of the primary ions.

The primary beam is focused to a much smaller spot size than the typical field of view of 1.5 × 1.5 mm^2 and scanned over the selected area. This ensures a homogeneous distribution of the ion fluence and enables laterally resolved analysis (imaging). Typical fluence for a single spectrum is 3 × 10^{13} He^+ ions/cm^2, thus for four different primary energies the total fluence is 1.2 × 10^{14} He^+ ions/cm^2. For the light He^+ ions this has a negligible influence on the LEIS signals (static analysis).

3. RESULTS AND DISCUSSION

3.1. Graphene Quality and Contamination. A complete analysis of the graphene/silicon system requires a sequence of well-defined sample preparation steps and data processing. The reduction of the surface contamination by annealing is shown in Figure 1. Here LEIS spectra are compared for 3 keV He^+ ions backscattered by a monolayer of graphene on a silicon substrate having a 3-nm-thick native oxide layer (section 2.2). For the as-deposited sample the only visible surface scattering peak is that of oxygen (~1100 eV). It results from the residual PMMA resist and other organic contaminants, such as alcohols on top of the graphene. The background below 1000 eV is due to sputtered ions. This background is so intense that it is difficult to identify the peak due to carbon (760 eV) under these conditions. As suggested by Cheng et al.,[21] most of this contamination is removed by heating the sample for 5 min at 400 °C in ultrahigh vacuum. No oxygen peak is present anymore, and the signal due to sputtered ions is strongly reduced. The clear carbon peak is present at its expected

DOI: 10.1021/acs.langmuir.5b01935
Langmuir 2015, 31, 9628−9635

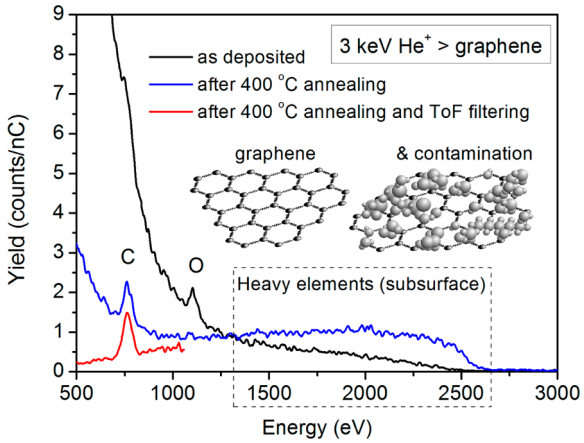

Figure 1. He^+ spectra (3 keV) for graphene: (i) as deposited and (ii) annealed at 400 °C for 5 min and measured without and with time-of-flight filtering, which reduces the background signal of the sputtered particles.

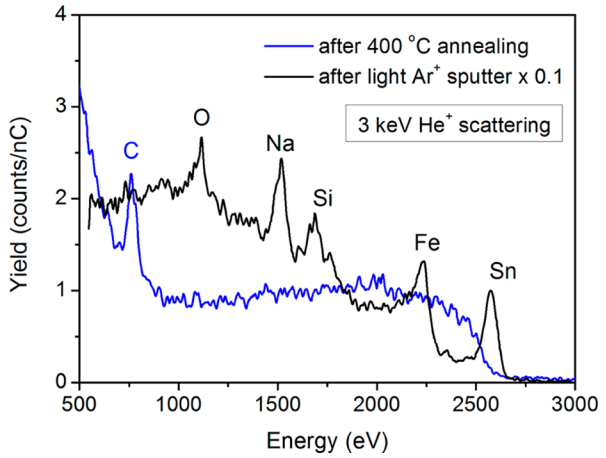

Figure 2. LEIS before and after partial removal of the graphene layer by Ar^+ sputtering (500 eV, ion fluence 3×10^{14} ions/cm^2).

position. For a given scattered ion energy the time of flight is determined by the mass of the ion. By using a pulsed ion beam and combining the energy analysis with ToF filtering of the ions arriving at the detector one can reject the sputtered (secondary) ions and selectively study He^+ (mass 4 amu). For the energy range of 500−1100 eV it is shown how this improves the detection and quantification of carbon.

Due to annealing, the background between 1500 and 2500 eV also becomes more intense. Its high-energy onset is much steeper than that one for the unheated sample, and no surface peaks can be detected in this energy range. Since the only surface peak is due to carbon, this proves the presence of a well-defined and pinhole-free carbon layer on top of the substrate.

The background in the (1500−2500) eV region results from He^+ ions that are backscattered by atoms below the outer surface and have lost additional energy. It is very unlikely that the ions have survived in their positive charge state; they rather have been reionized before leaving the surface. Since the onset is much higher in energy than expected for silicon and oxygen, this background must be due to contamination by much heavier elements. These heavier elements (along with sodium) are intercalated at the graphene−silicon interface, thus just below the graphene. They are easily revealed in the LEIS spectrum after the removal of a significant fraction of the graphene monolayer by low-fluence argon sputtering (500 eV Ar^+, under 59°, ion fluence 3×10^{14} ions/cm^2) (Figure 2). Alternatively, the graphene can be removed by oxidation with atomic oxygen. The identities of the detected heavy elements (Fe and Sn) were confirmed by 5 keV Ne^+ scattering. Neon gives a much better mass resolution than helium for these elements.

For other samples having a graphene double layer, we quantified the amounts of Fe and Sn after atomic oxygen oxidation by calibration against oxidized Fe and Sn samples. The surface coverages were found to be up to 15 and 30% for Fe and Sn, respectively. These contaminants were also detected by RBS (200 keV deuterons). Although the in-depth resolution at higher ion energies of RBS is much worse (14 nm) than for LEIS, the simulation of the tin and iron signals in RBS shows that the signals result from a thin layer close to the graphene−silicon oxide interface.

The observed elements and their coverages are, of course, specific to the way that the samples have been prepared. It is worrying, however, that we found that a total coverage of intercalated heavy elements of 10−50% is not unusual for such graphene samples. A batch of commercial graphene, studied for comparison, showed a comparable quantity of metallic impurities in subsurface layers, in addition to the presence of chlorine in the top atomic layer prior to annealing. Also, there was a significant Si signal from the commercial graphene after annealing, which could be due to either holes in the graphene or to siloxane contamination.

The presence of such large fractions of heavy elements will have a significant and uncontrollable effect on the electronic properties of the graphene layer.[13] When other surface analytical techniques such as XPS are used, the information depth is much larger than one atomic layer. This dilutes the observed concentration significantly. Since the LEIS instrument applied in this study has a much higher sensitivity, it has been used as the analytical tool of choice in the optimization of the synthesis procedure.

3.2. Origin of Iron and Tin Contamination. The iron contamination originates from the technology of the CVD graphene preparation, when the supporting copper foil is etched away by the oxidant−etchant solution (in our case an aqueous solution of $Fe(NO_3)_3$), as has already been reported.[12]

The graphene contamination by tin can originate from numerous possible sources. Tin is readily soluble in copper, as can be seen from the phase diagram.[27] It forms stable alloys which have been well known for many centuries. Even though the copper foil used to grow the graphene was of high purity, it still contains traces of other elements or it can be easily contaminated by tin during graphene preparation at elevated temperatures. The presence of tin in the used copper foil is clearly identified by SIMS depth profiling (Supporting Information). The origin of tin contamination will be the subject of further investigation.

During the selective etching of copper in an aqueous solution of $Fe(NO_3)_3$, the tin originally present in the whole copper foil (25 μm thick) can be concentrated and deposited on the bottom side of the graphene. Consequently, tin may form an intercalated contamination at the graphene−silica interface, where it was localized by LEIS.

3.3. Identification of Carbon Hybridization. The presence of a pinhole-free carbon film at the top of the analyzed sample does not automatically identify graphene as the only possible allotrope of carbon in this film. For the

DOI: 10.1021/acs.langmuir.5b01935
Langmuir 2015, 31, 9628−9635

identification (electronic structure−hybridization) and quantification of carbon in graphene and in organic contaminants the energy dependence of the neutralization of the scattered He^+ ions is used. A highly ordered pyrolytic graphite (HOPG, long-range sp^2 hybridization) and silicone rubber (sp^3 hybridization) are used as the reference samples for graphitic and nongraphitic (other) forms of carbon, respectively. In addition, a reference polycrystalline copper sample is used to determine the instrumental factor of the apparatus. Figure 3 shows the LEIS

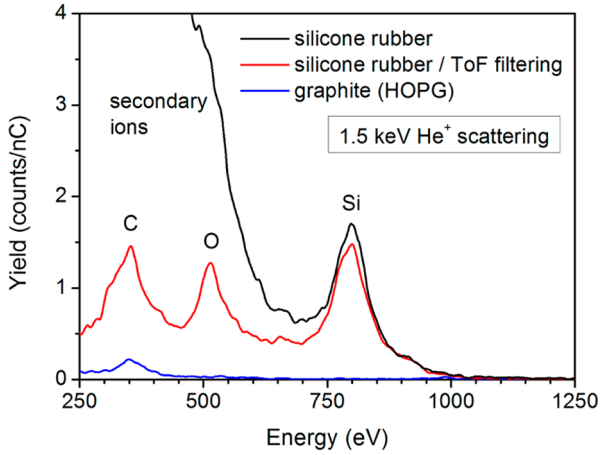

Figure 3. LEIS signal of the reference samples (graphite (HOPG) and silicone rubber). ToF filtering reduces the background signal of the sputtered particles.

spectra for 1.5 keV He^+ scattered from silicone rubber and graphite. In the former case, the spectra were recorded without and with ToF filtering to suppress the secondary ions.

The carbon peak of silicone rubber is much larger than that of graphite. This is counterintuitive, since the surface density of carbon is about 1 order of magnitude larger in graphite than in silicone rubber. The origin of this paradox is an exceptionally strong matrix effect in the neutralization of helium ions by carbon. This was discovered in 1994 for carbon on rhenium.[22,23] By changing the temperature (1800−2000 K) of a carbon-doped rhenium sample the surface could be changed (reversibly) from multilayer graphite via monolayer graphite to carbidic (nongraphitic submonolayer) carbon. In this way the effects of neutralization and the scattering cross section could be studied independently, since the latter is the same for all forms of carbon hybridization. A similar idea is used in our work on graphene presented here. The graphene neutralization is expected to follow the graphite trend while carbon in organic (nongraphitic) contaminants should give neutralization results similar to that of silicone rubber.

An additional advantage of the high-temperature treatment of rhenium was that any damage caused by ion beam sputtering was immediately annealed out. Thus, high ion fluences could be applied. In the present experiments the use of the high-sensitivity double toroidal energy analyzer allows us to use such low ion fluences that graphene can be studied at room temperature without detectable damage.

The ion yield per unit of primary charge, S_i, backscattered from the surface atoms i is a measure of the atomic surface concentration[20] (number density of surface atoms) n_i

$$S_i = n_i \frac{d\sigma_i}{d\Omega} P_i^+ c \qquad (1)$$

where $d\sigma_i/d\Omega$ is the differential scattering cross section for scattering by an element i and c is the instrumental factor, taking into account the solid angle of acceptance of the analyzer, the detector efficiency, and the analyzer transmission. For the analyzer used in the present study the instrumental factor is independent of the energy of the ions. P_i^+ is the ion fraction of the He scattered by element i.

The scattering cross section, which is determined by the screened nucleus of the carbon atom and not by its valence electrons, has been calculated with the Thomas−Fermi−Moliere potential.[28] The ion fraction P_i^+ of the backscattered helium particles is given by[20]

$$P_i^+ = \exp\left(\frac{-v_{c_i}}{v}\right) \qquad (2)$$

where $1/v = 1/v_i + 1/v_f$ is the inverse velocity, v_i and v_f are the ion velocities before and after the collision, and v_{c_i} is the characteristic velocity for a given ion−target atom (i) combination. The characteristic velocity is a measure of the neutralization strength.

The ion fraction, which is thus the crucial parameter for the observed matrix effect, can be determined by plotting the logarithm of $S_i/(c\ d\sigma_i/d\Omega)$ against the inverse velocity. In Figure 4 this is shown for (1.5−10 keV) He^+ scattering by

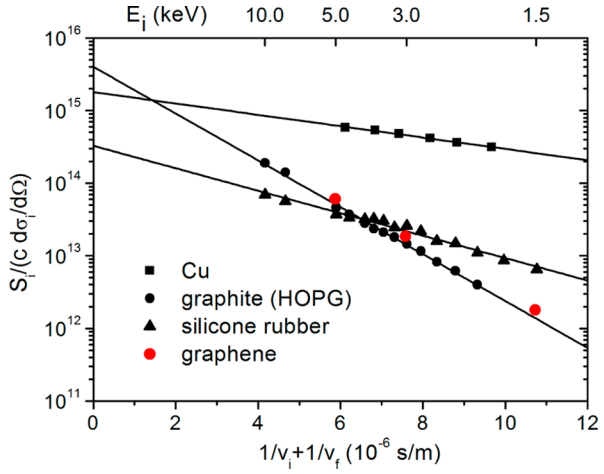

Figure 4. Plot of $\ln(S_i/(c\ d\sigma_i/d\Omega))$ versus the inverse velocity for He^+ scattering by Cu and by carbon in graphite (HOPG), silicon rubber, and graphene. Drawn black lines are fits for Cu, graphite, and silicone rubber. The corresponding primary energy range (1.5−10.0 keV) is indicated for helium−carbon collisions on the top axis.

graphite, silicone rubber, and graphene and for 1−2.5 keV scattering by Cu. For all of the samples this gives a straight line similar to those in Figure S2 in Supporting Information. The advantage of Figure 4 presented here is that the extrapolated values for infinite velocities $(1/v = 0)$ are the logarithms of n_i. Thus, the intercept of each line with the vertical axis indicates the atomic surface concentration for each material. Using the polycrystalline Cu sample (1.8×10^{15} atoms/cm^2) as a reference,[22,29] the surface densities of carbon for graphite and silicone rubber were determined to be 3.8 and 0.33×10^{15} atoms/cm^2, respectively. For the graphene sample the slope and the y-axis intersection are nearly the same as those for graphite. Thus, the ion neutralization and the atom density in the outer surfaces for the reference graphite and graphene samples are the same. All data are taken at such low fluence

DOI: 10.1021/acs.langmuir.5b01935
Langmuir 2015, 31, 9628−9635

(static conditions) that the damage by the ion beam is negligible (Supporting Information). For higher fluences or impact with heavier ions, significant sputtering and damage will occur. For graphite and graphene this will change the electronic structure near the defects. Since there is now a mixture of two types of carbon, there is no longer a straight line for plots such as that shown in Figure 4. In particular, at very low energies the LEIS signal becomes much stronger. For instance, when bombarding the surface with 500 eV Ar^+ ions (at 59°) there is already a detectable change in the plot for a fluence that is $\geq 1 \times 10^{14}$ ions/cm^2.

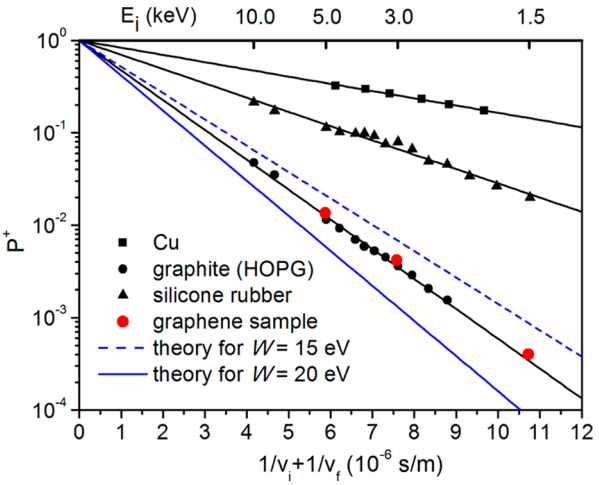

Figure 5. Plot of P^+ versus $(1/v_i + 1/v_f)$ for Cu, graphite (HOPG), silicone rubber, and graphene. Drawn black lines are fits for Cu, graphite, and silicone rubber. All lines meet at $P^+ = 1$, where the interaction time offered for neutralization is infinitely small. The blue lines are the theoretical predictions (eq 4) for bandwidths W of 15 and 20 eV. For an effective bandwidth of 17.1 eV the prediction coincides with the experiments for graphite and graphene.

Figure 5 is obtained from Figure 4 by correcting the data for the atomic densities. The characteristic velocities v_{c_i} for scattering by carbon in graphene/graphite and in silicone rubber are $(7.4 \pm 0.1) \times 10^5$ and $(3.6 \pm 0.2) \times 10^5$ m/s, respectively. The theoretical predictions (see below) are also given for scattering by a sample having valence bandwidths W of 15 and of 20 eV.

In practice, the surface of graphene samples often consists of a mixture of graphene and organic contaminants. For instance, it is known that cleaning with acetone cannot completely remove resist residues due to their strong van der Waals interaction with graphene.[21] For such a mixture a plot such as that in Figure 4 or 5 will not produce a straight line. Depending on the actual surface fractions, the high-energy part (at low values of $1/v_i + 1/v_f$) will be dominated by the graphene fraction, while as a result of its low neutralization probability the nongraphene carbon will prevail at low energies (at high values of $1/v_i + 1/v_f$), as can be seen in Figure S3 in the Supporting Information. As shown in this figure, a surface fraction of 3 atom % nongraphene carbon can still be detected on a graphene surface. This defines the detection limit for nongraphene carbon on top of graphene for the instrumentation used (1.1×10^{14} atoms/cm^2).

It is known[21,30] that heating the graphene samples in an Ar/H_2 flow at 400 °C results in the complete removal of the resist contamination of a graphene surface. In the present study the LEIS analysis shows that the organic contamination can also be fully removed by heating in UHV at 400 °C for 5 min. The 400 °C heat treatment induces, however, an increased coupling between the graphene and the underlying SiO_2 substrate which leads to severe degradation of the charge mobilities in graphene devices.[21] Therefore, other treatments, such as a chemical one based on chloroform, may be advantageous.[21]

For some ion−sample combinations the neutralization of the backscattered He^+ depends on the chemical state of the target atom. Such matrix effects are known,[20] for example, for surfaces having a very low work function, for elements where quasi-resonant neutralization is possible (He^+ scattering by Pb, Bi, Ga, and In), and for several metallic surfaces such as NiAl (110)[31] and Cu.[32] In comparison to these cases, the observed matrix effect for carbon is significantly larger as at 1.5 keV He^+ scattering the ion fraction for graphene and graphite is a factor of 50 lower than that for carbon in nongraphitic (carbidic or organic) forms of carbon. Two possible origins of this unique matrix effect are discussed below.

3.4. Resonant Charge Transfer. The most efficient neutralization process is resonant charge transfer, as discovered by Ziemba and Everhart in 1959.[33] Since then it has been known that this process is responsible for the very efficient charge transfer in wide-angle scattering between a helium ion projectile and a helium target atom. In this case the charge transfer is fully symmetric (no energy is lost or gained during the electron transfer). Therefore, classically speaking, the electron will oscillate between the helium particles during their interaction time T. Exact resonance is not required for this process. Thus, when there is an energy mismatch (quasi-resonance) ΔE between the He level and the level in the target, the energy loss or gain is compensated for by a transfer of kinetic energy of the nuclei to electronic energy (or vice versa).

The influence of the energy mismatch is independent of the sign and thus the same for energy loss and gain. The smaller $|\Delta E|$ and the higher E_0, the more likely is this process.[34] Also, in the close collision during the backscattering of keV ions, the helium 1s level shifts significantly as a function of the ion−atom distance.[35] Experimentally it has been found that for E_0 as low as 500 eV, charge transfer can still be significant for $|\Delta E| < 10$ eV.[36]

For He^+ (1s level) scattering by Pb (5d level) such an accidental quasi-resonance exists. The 5d electron can transfer to the 1s hole in He^+. If the interaction time T is long enough, then the electron can also transfer back to the 5d hole depending on T and thus on the velocity of the He projectile, and the scattered He is charged with varying probability. Therefore, this resonance leads to strong oscillations in the scattered ion yield as a function of the primary energy in the energy range of 0.2−2 keV.[37,38] Whenever a (quasi-) resonant neutralization is possible, it is so efficient that other processes such as Auger neutralization can be neglected.[39−42]

Charge exchange between He^+ ions and graphite is a very efficient and fast process.[22,23,41,43,44] Since the He 1s level is resonant with the electronic states in the wide sp^2 band of graphite (HOPG),[45] it is generally accepted that this efficient neutralization results from resonant neutralization. Recent calculations by the group of Goldberg[41] give a detailed quantum mechanical description in which a carbon atom and its nearest neighbors are included. The results suggest that the

DOI: 10.1021/acs.langmuir.5b01935
Langmuir 2015, 31, 9628−9635

resonant neutralization is not only with the ground state but also involves important contributions from excited states of He. For 5 keV He^+ scattering by 135° the calculated neutral fraction is 0.93, which is in good agreement with their experimental value of 0.95 as well as our value of 0.98 ± 0.01. However, within their primary energy range (1−6 keV) the theoretical ion fraction is more or less independent of the primary energy. Also, (weak) oscillations are clearly visible. This is in contrast to our experimental results (Figure 5) and the earlier results of Van den Oetelaar et al.[22] and Mikhailov et al.,[23] where the ion fraction for graphite at 1.5 keV is about 60 times lower than at 6 keV. We believe that this discrepancy between theory and experiment is due to a much stronger damping of the resonant transfer than what is included in the theory of Iglesias-Garcia.[41]

3.5. Resonant Charge Transfer with Damping. There are two important factors that lead to damping of the oscillatory charge transfer between a single state (He, 1s) and the states of an energy band: destructive interference and the short lifetime of a vacancy in the valence band.

The two-state approximation that holds for resonant charge exchange between two degenerate states breaks down when additional states are mixed in. This destroys the interference. Lichten[46,47] gave a quantum mechanical estimate for the decay time Δt of the damping of the (quasi-) resonant electron oscillation between an ion and a filled band (full width W) which may be used to determine the probability of the projectile to survive in its charged state

$$\Delta t = \frac{\pi}{W} \tag{3}$$

where the parameters are in atomic units. According to this model the ion fraction after scattering is

$$P^+ = e^{-T/\Delta t} \tag{4}$$

The experimental density of valence states of graphite (HOPG) and of graphene has a full width of approximately 20−25 eV.[45] Theoretical predictions for graphene give a somewhat smaller width of 20 eV.[48]

For the scattering of a He^+ ion by a carbon atom the interaction time T can be estimated using its classical trajectory. For 3 keV ions and a scattering angle of 145°, $T \approx 7 \times 10^{-16}$ s, which gives for a bandwidth of 20 eV an ion fraction of $P^+ = 1.4 \times 10^{-3}$. This is comparable to the experimental value (3.6×10^{-3}) (Figure 5).

When the energy mismatch between the He 1s level and a level in the graphene band is large, the quasi-resonant electron transfer will be slow. Thus, levels in the band that are far away from the He 1s level cannot contribute to the destruction of the interference. Quasi-resonant charge transfer has been observed[36] for $|\Delta E| < 10$ eV. Therefore, it seems reasonable to assume the same limit for destructive interference. Even after taking into account the shift of the He 1s level by the interaction with graphene and if one would use the theoretical instead of the experimental bandwidth, He 1s will not be located at the center of the band. The effective bandwidth will thus be between 10 and 20 eV. In Figure 5 the predictions are given for bandwidths of 15 and 20 eV. An exact agreement with experiment would be reached for an effective bandwidth of 17.1 eV.

During the He^+−HOPG interaction time an electron from a level in the band can be transferred to the He^+. The resulting hole in the band then diffuses in the band with a diffusion time that is almost equal to the reciprocal of the bandwidth,[43] thus the wider the band, the faster the hole diffuses away. When the hole is transferred, it cannot return to the He^+ anymore ("it has disappeared in the band" and is thus not available). Therefore, for the (quasi-) resonant interaction of He^+ with the very wide band of graphite or graphene, resonant charge transfer represents an effective neutralization mechanism, and it works only one way (Figure 6)—by strong damping of the oscillation.

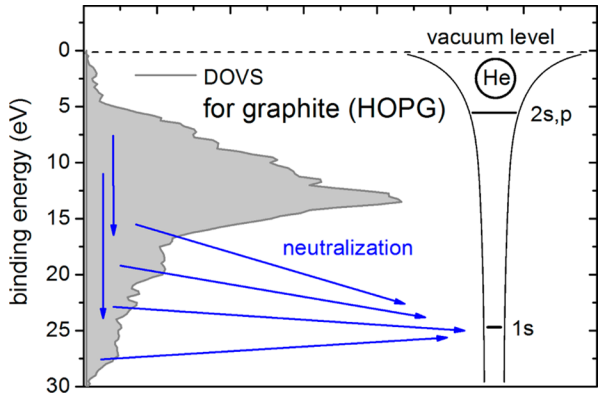

Figure 6. Experimental density of the valence states of graphite (HOPG)[49] and the ground state of He. The He^+ ion is effectively neutralized by an electron of the graphite band. Both destructive interference and diffusion in the valence band contribute to the neutralization.

Hence both the time for destructive interference and the short lifetime of the hole in the valence band scale with the reciprocal of the bandwidth. This dependence has also been found by Kondo[50] using quantum rate equations, although his results were for primary energies below 1 keV. The exceptionally strong neutralization of helium ions by graphite and graphene is thus the result of the fact that the band of graphene (and graphite) extends to such low energies that it is in (or nearly in) energy resonance with the He 1s level (Figure 6). Especially for the lower primary energies (longer interaction times) this leads to very low ion fractions, making the detection of this type of carbon very difficult at energies below 2 keV. For carbon atoms in nongraphitic form (organic molecules or carbidic carbon) there is not such an energy band and resonance with the He 1s level. Therefore, the ion fraction is much higher.

4. SUMMARY

CVD graphene transferred on thermal silica/silicon substrates is analyzed by high-sensitivity LEIS with parallel energy analysis and ToF filtering for background reduction. Thanks to the high sensitivity and extraordinary depth resolution typical of LEIS the closure of the graphene layer is confirmed. Different kinds of contaminants are detected, quantified, and localized within the graphene structure. First, the residual resist and other types of organic adsorbates are reduced by thermal treatment under UHV conditions. Then, carbon in graphene is distinguished from that in nongraphitic forms by performing LEIS experiments at different primary ion energies. Here, the extraordinarily strong neutralization of He^+ by the graphene carbon atoms is utilized. Two models are discussed to explain the difference in neutralization. Both are based on a quasi-resonant charge transfer of an electron from the very wide energy band of graphene to the helium 1s vacancy. Also, for both, the ion

DOI: 10.1021/acs.langmuir.5b01935
Langmuir 2015, 31, 9628−9635

fraction of the scattered ions depends exponentially on the width of the energy band.

Additional experiments confirmed that the samples have compact, pinhole-free, graphene layers contaminated by metal impurities such as Fe, Sn, and Na (total coverage of metal impurities for up to 50% of a monolayer). These impurities are introduced during the synthesis of the CVD graphene and the transfer onto the substrates. These elements are localized at the graphene−silica interface (i.e., they were intercalated just below the graphene).

Hence, high-resolution low-energy ion scattering offers a unique combination of surface sensitivity, depth resolution, and quantification. It is capable of both checking the cleanliness of graphene surfaces (e.g., the degree of contamination by the remnants of resists) and detecting impurities incorporated into graphene layers or their interfaces (intercalation). Thus, it is an effective method for monitoring the quality of the whole fabrication process of graphene, including its transfer onto various substrates.

■ ASSOCIATED CONTENT

Supporting Information

The Supporting Information is available free of charge on the ACS Publications website at DOI: 10.1021/acs.langmuir.5b01935.

SIMS depth profiles of copper foil used for graphene growth. Plot of $\ln(S_i/(d\sigma_i/d\Omega))$ versus the inverse velocity for He^+ scattering by Cu and by carbon in graphite, silicon rubber, and graphene. Calculated plots of $S_i/(c\ d\sigma_i/d\Omega))$ versus the inverse velocity. ToF-LEIS spectrum of a graphene-on-silica sample measured with a conventional spectrometer. (PDF)

■ AUTHOR INFORMATION

Corresponding Author

*E-mail: H.H.Brongersma@tue.nl.

Notes

The authors declare no competing financial interest.

■ ACKNOWLEDGMENTS

This work was supported by ION-TOF GmbH, AKTION programme 70p10, and CEITEC. We thank Ing. Radek Duda, Ing. Josef Polčák, Ph.D., Ing. Michal Potoček, Ph.D., DI Dominik Göbl, Ph.D., Barbara Bruckner, and Prof. Dr. Peter Zeppenfeld for supporting discussions and collaboration in graphene preparation and XPS, AES, and RBS analysis. We acknowledge support from the European Regional Development Fund (CEITEC CZ.1.05/1.1.00/02.0068) and the Technology Agency of the Czech Republic (grant no. TE01020233).

■ REFERENCES

(1) Mayorov, A. S.; Elias, D. C.; Mukhin, I. S.; Morozov, S. V.; Ponomarenko, L. A.; Novoselov, K. S.; Geim, A. K.; Gorbachev, R. V. How Close Can One Approach the Dirac Point in Graphene Experimentally? *Nano Lett.* **2012**, *12*, 4629−4634.

(2) Giesbers, A. J. M.; Uhlirova, K.; Konecny, M.; Peters, E. C.; Burghard, M.; Aarts, J.; Flipse, C. F. J. Interface-Induced Room-Temperature Ferromagnetism in Hydrogenated Epitaxial Graphene. *Phys. Rev. Lett.* **2013**, *111*, 166101.

(3) Novoselov, K. S.; Fal'ko, V. I.; Colombo, L.; Gellert, P. R.; Schwab, M. G.; Kim, K. A roadmap for graphene. *Nature* **2012**, *490*, 192−200.

(4) Schedin, F.; Geim, A. K.; Morozov, S. V.; Hill, E. W.; Blake, P.; Katsnelson, M. I.; Novoselov, K. S. Detection of Individual Gas Molecules Adsorbed on Graphene. *Nat. Mater.* **2007**, *6*, 652−655.

(5) Fowler, J. D.; Allen, M. J.; Tung, V. C.; Yang, Y.; Kaner, R. B.; Weiller, B. H. Practical Chemical Sensors from Chemically Derived Graphene. *ACS Nano* **2009**, *3*, 301−306.

(6) Avdoshenko, S. M.; Nozaki, D.; da Rocha, C. G.; González, J. W.; Lee, M. H.; Gutierrez, R.; Cuniberti, G. Dynamic and Electronic Transport Properties of DNA Translocation through Graphene Nanopores. *Nano Lett.* **2013**, *13*, 1969−1976.

(7) Gan, X.; Shiue, R. J.; Gao, Y.; Meric, I.; Heinz, T. F.; Shepard, K.; Hone, J.; Assefa, S.; Englund, D. Chip-Integrated Ultrafast Graphene Photodetector with High Responsivity. *Nat. Photonics* **2013**, *7*, 883−887.

(8) Bonaccorso, F.; Sun, Z.; Hasan, T.; Ferrari, A. C. Graphene photonics and optoelectronics. *Nat. Photonics* **2010**, *4*, 611−622.

(9) Schneider, G. F.; Kowalczyk, S. W.; Calado, V. E.; Pandraud, G.; Zandbergen, H. W.; Vandersypen, L. M. K.; Dekker, C. DNA Translocation through Graphene Nanopores. *Nano Lett.* **2010**, *10*, 3163−3167.

(10) Banhart, F.; Kotakoski, J.; Krasheninnikov, A. V. Structural Defects in Graphene. *ACS Nano* **2011**, *5*, 26−41.

(11) Lin, Y.-C.; Lu, C.-C; Yeh, C.-H.; Jin, C.; Suenaga, K.; Chiu, P.-W. Graphene Annealing: How Clean Can It Be? *Nano Lett.* **2012**, *12*, 414−419.

(12) Ambrosi, A.; Pumera, M. The CVD Graphene Transfer Procedure Introduces Metallic Impurities which Alter the Graphene Electrochemical Properties. *Nanoscale* **2014**, *6*, 472−476.

(13) Krasheninnikov, A. V.; Nieminen, R. M. Attractive Interaction between Transition-Metal Atom Impurities and Vacancies in Graphene: A First-Principles Study. *Theor. Chem. Acc.* **2011**, *129*, 625−630.

(14) Liang, X.; Sperling, B. A.; Calizo, I.; Cheng, G.; Hacker, C. A.; Zhang, Q.; Obeng, Y.; Yan, K.; Peng, H.; Li, Q.; Zhu, X.; Yuan, H.; Walker, A. R. H.; Liu, L.; Richter, C. Toward Clean and Crackless Transfer of Graphene. *ACS Nano* **2011**, *5*, 9144−9153.

(15) Ma, D.; Zhang, Y.; Liu, M.; Ji, Q.; Gao, T.; Zhang, Y.; Liu, Z. Clean Transfer of Graphene on Pt Foils Mediated by a Carbon Monoxide Intercalation Process. *Nano Res.* **2013**, *6*, 671−678.

(16) Lupina, G.; Kitzmann, J.; Costina, I.; Lukosius, M.; Wenger, C.; Wolff, A.; Vaziri, S.; Ostling, M.; Pasternak, I.; Krajewska, A.; Strupinski, W.; Kataria, S.; Gahoi, A.; Lemme, M. C.; Ruhl, G.; Zoth, G.; Luxenhofer, O.; Mehr, W. Residual Metallic Contamination of Transferred Chemical Vapor Deposited Graphene. *ACS Nano* **2015**, *9*, 4776−4785.

(17) Aleman, B.; Regan, W.; Aloni, S.; Altoe, V.; Alem, N.; Girit, C.; Geng, B.; Maserati, L.; Crommie, M.; Wang, F.; Zettl, A. Transfer-Free Batch Fabrication of Large-Area Suspended Graphene Membranes. *ACS Nano* **2010**, *4*, 4762−4768.

(18) Li, X. S.; Cai, W. W.; An, J. H.; Kim, S.; Nah, J.; Yang, D. X.; Piner, R. D.; Velamakanni, A.; Jung, I.; Tutuc, E.; Banerjee, S. K.; Colombo, L.; Ruoff, R. S. Large-Area Synthesis of High Quality and Uniform Graphene Films on Copper Foils. *Science* **2009**, *324*, 1312−1314.

(19) Brongersma, H. H.; Low-Energy Ion Scattering. In *Characterization of Materials*; Kaufmann, E. N., Ed.; Wiley, 2012; pp 2024−2044.

(20) Brongersma, H. H.; Draxler, M.; de Ridder, M.; Bauer, P. Surface Composition Analysis by Low-Energy Ion Scattering. *Surf. Sci. Rep.* **2007**, *62*, 63−109.

(21) Cheng, Z.; Zhou, Q.; Wang, C.; Li, Q.; Wang, C.; Fang, Y. Toward Intrinsic Graphene Surfaces: A Systematic Study on Thermal Annealing and Wet-Chemical Treatment of SiO2-Supported Graphene Devices. *Nano Lett.* **2011**, *11*, 767−771.

(22) van den Oetelaar, L. C. A.; Mikhailov, S. N.; Brongersma, H. H. Mechanism of Neutralization in Low-Energy He+ Ion Scattering from Carbidic and Graphitic Carbon Species on Rhenium. *Nucl. Instrum. Methods Phys. Res., Sect. B* **1994**, *85*, 420−423.

DOI: 10.1021/acs.langmuir.5b01935
Langmuir 2015, 31, 9628−9635

(23) Mikhailov, S. N.; van den Oetelaar, L. C. A.; Brongersma, H. H. Strong Matrix Effect in Low-Energy He+ Ion Scattering from Carbon. *Nucl. Instrum. Methods Phys. Res., Sect. B* **1994**, *93*, 210−214.
(24) Zeng, J.; Yao, H. J.; Zhang, S. X.; Zhai, P. F.; Duan, J. L.; Sun, Y. M.; Li, G. P.; Liu, J. Swift Heavy Ions Induced Irradiation Effects in Monolayer Graphene and Highly Oriented Pyrolytic Graphite. *Nucl. Instrum. Methods Phys. Res., Sect. B* **2014**, *330*, 18−23.
(25) Krasheninnikov, A. V.; Nordlund, K. Ion and Electron Irradiation-Induced Effects in Nanostructured Materials. *J. Appl. Phys.* **2010**, *107*, 071301.
(26) Kolibal, M.; Pusa, S.; Babor, P.; Mach, J.; Sikola, T. TOF-LEIS Analysis of Ultra Thin Films: Ga and Ga-N Layer Growth on Si(111). *Surf. Sci.* **2004**, *566-568*, 885−889.
(27) Fürtauer, S.; Li, D.; Cupid, D.; Flandorfer, H. The Cu-Sn Phase Diagram, Part I: New Experimental Results. *Intermetallics* **2013**, *34*, 142−147.
(28) Ziegler, J. F.; Biersack, J. P.; Littmark, U. *The Stopping and Range of Ions in Solids*; Pergamon: New York, 1985; Vol. *1*.
(29) Primetzhofer, D.; Markin, S. N.; Juaristi, J. I.; Taglauer, E.; Bauer, P. Crystal Effects in the Neutralization of He(+) Ions in the Low Energy Ion Scattering Regime. *Phys. Rev. Lett.* **2008**, *100*, 213201.
(30) Ishigami, M.; Chen, J. H.; Cullen, W. G.; Fuhrer, M. S.; Williams, E. D. Atomic Structure of Graphene on SiO_2. *Nano Lett.* **2007**, *7*, 1643−1648.
(31) Jacobs, J. P.; Reijne, S.; Elfrink, R. J. M.; Mikhailov, S. N.; Brongersma, H. H.; Wuttig, M. Quantification of the Composition of Alloy and Oxide Surfaces Using Low-Energy Ion Scattering. *J. Vac. Sci. Technol., A* **1994**, *12*, 2308−2313.
(32) Draxler, M.; Gruber, R.; Brongersma, H. H.; Bauer, P. Velocity Scaling of Ion Neutralization in Low Energy Ion Scattering. *Phys. Rev. Lett.* **2002**, *89*, 263201.
(33) Ziemba, F. P.; Everhart, E. Resonance Phenomena in Large-Angle Helium Ion-Helium Atom Collisions. *Phys. Rev. Lett.* **1959**, *2*, 299−301.
(34) Hasted, J. B. *Physics of Atomic Collisions*; Elsevier: New York, 1972; Chapter 12.
(35) Monreal, R. C.; Goebl, D.; Primetzhofer, D.; Bauer, P. Effects of the Atomic Level Shift in the Auger Neutralization Rates of Noble Metal Surfaces. *Nucl. Instrum. Methods Phys. Res., Sect. B* **2013**, *315*, 206−212.
(36) Rusch, T. W.; Erickson, R. L. Energy Dependence of Scattered Ion Yields in ISS. *J. Vac. Sci. Technol.* **1976**, *13*, 374−377.
(37) Erickson, R. L.; Smith, D. P. Oscillatory Cross Sections in Low-Energy Ion Scattering from Surfaces. *Phys. Rev. Lett.* **1975**, *34*, 297−299.
(38) Brongersma, H. H.; Buck, T. M. Neutralisation Behavior in Scattering of Low Energy Ions from Solid Surfaces. *Nucl. Instrum. Methods* **1976**, *132*, 559−564.
(39) Silva, J. A. M. C.; Wolfgang, J.; Borisov, A. G.; Gauyacq, J. P.; Nordlander, P.; Teillet-Billy, D. Resonant Charge Transfer Process in Ion-Metal Surface Collisions: Effect of the Presence of Vacancies on the Surface. *Nucl. Instrum. Methods Phys. Res., Sect. B* **1999**, *157*, 55−60.
(40) Bajales Luna, N.; Bonetto, F. J.; Vidal, R. A.; Goldberg, E. C.; Ferron, J. Low Energy Ion Scattering in He/HOPG System. *J. Mol. Catal. A: Chem.* **2008**, *281*, 237−240.
(41) Iglesias-García, A.; García, E. A.; Goldberg, E. C. Role of He Excited Configurations in the Neutralization of He+ Ions Colliding with a HOPG Surface. *Phys. Rev. B: Condens. Matter Mater. Phys.* **2013**, *87*, 075434.
(42) Goebl, D.; Roth, D.; Primetzhofer, D.; Monreal, R. C.; Abad, E.; Putz, A.; Bauer, P. Quasi-Resonant Neutralization of He+ Ions at a Germanium Surface. *J. Phys.: Condens. Matter* **2013**, *25*, 485006.
(43) Tsuneyuki, S.; Shima, N.; Tsukada, M. Band effect on the charge exchange process at solid surfaces. *Surf. Sci.* **1987**, *186*, 26−44.
(44) Souda, R.; Yamamoto, K. Band Effect on Resonance Neutralization. *Nucl. Instrum. Methods Phys. Res., Sect. B* **1997**, *125*, 256−261.
(45) Khvostov, V. V.; Babaev, V. G.; Dementjeva, E. A.; Guseva, M. B. Electronic Structure of Cs-Graphite Surface Studied by Auger-Spectroscopy. *Surf. Sci.* **1996**, *345*, L44−L48.
(46) Lichten, W. Resonant Charge Exchange in Atomic Collisions. *Phys. Rev.* **1963**, *131*, 229−238.
(47) Lichten, W. Resonant Charge Exchange in Atomic Collisions. II Further Applications and Extension to the Quasi-Resonant Case. *Phys. Rev.* **1965**, *139*, A27−A34.
(48) Nakada, K.; Ishii, A. DFT Calculation for Adatom Adsorption on Graphene. In *Graphene Simulation*; Gong, J. R., Ed.; InTech Publisher, 2011.
(49) Reprinted from Results and Discussion section of Khvostov, V. V.; Babaev, V. G.; Dementjeva, E. A.; Guseva, M. B. Electronic Structure of Cs-Graphite Surface Studied by Auger-Spectroscopy. *Surf. Sci.* **1996**, *345*, L46 with permission from Elsevier (Copyright (1996)).
(50) Kondo, S. Influence of Band Width on the Scattered Ion Yield Spectra of a He+ Ion by Resonant or Quasi-Resonant Charge Exchange Neutralization. *J. Phys. Soc. Jpn.* **2011**, *80*, 044717.

DOI: 10.1021/acs.langmuir.5b01935
Langmuir 2015, 31, 9628−9635